IEEE Access
Multidisciplinary | Rapid Review | Open Access Journal

Received March 26, 2018, accepted May 8, 2018, date of publication May 21, 2018, date of current version June 19, 2018.

Digital Object Identifier 10.1109/ACCESS.2018.2838523

Hybrid Full-Duplex and Alternate Multiple Relay Selection and Beamforming in AF Cooperative Networks

LUTFI SAMARA, ALA GOUISSEM, AND RIDHA HAMILA
Department of Electrical Engineering, Qatar University, Doha 2713, Qatar

Corresponding author: Lutfi Samara (samara@qu.edu.qa)

This work was supported by the Qatar National Research Fund (a member of the Qatar Foundation) through GSRA under Grant #2-1-0601-14011.

ABSTRACT In this paper, multiple relay selection and beamforming techniques are applied to a dual-hop full-duplex (FD) amplify-and-forward relaying network. We show that our proposed techniques allow the selection to be adaptive to the residual self-interference (SI) level for each of the available relays in the network. The adaptivity of our selection schemes is manifested through a hybrid system that is based on FD relaying and switching based on the overall channel conditions and the statistics of the residual SI channel for each of the relays. In particular, different proposed techniques are shown to be able to adaptively decide on when and how often the used relays should be switched in the case of overwhelming residual SI. Our results show that allowing such a fusion considerably improves the overall performance of the considered relaying scheme in terms of bit error rate compared with state-of-the-art relay selection schemes.

INDEX TERMS Relaying, beamforming, amplify-and-forward, full-duplex, node switching.

I. INTRODUCTION

In order to cope with the increasing demand on wireless communication applications, the next generation wireless communication standard in its fifth generation (5G) issue is set to fulfill the aims of supporting high data rate and reliable wireless communications. Moreover, improving the spectral efficiency of wireless communication networks increases the network capacity, which partially fulfills the aims of 5G.

Several methods have been introduced to achieve a higher spectral efficiency, and one of the most interesting techniques was the use of full-duplex (FD) radio transceivers. Theoretically, a FD transceiver is able to double the spectral efficiency compared with half duplex (HD) transceivers by simultaneously transmitting and receiving data at the same frequency band [1]–[3]. This is possible when the FD transceiver possesses self-interference (SI) cancelation capabilities [1], [4], [5]. SI emerges due to the usage of the same time and frequency resources, which was always avoided by the conventional method of orthogonalizing the resources. Furthermore, the use of data relaying between a source and a destination has proved to be an effective approach to increase the diversity of wireless communication signals, therefore improving the overall reliability and performance of wireless networks.

Basically, relaying adopts two types of protocols: Amplify-and-forward (AF) and decode-and-forward (DF) protocols [6], [7]. The AF protocol allows the relay to re-transmit the received information while just amplifying it from the source to the destination, while the DF protocol allows the relay to decode the received information before forwarding it to the destination. For the case of AF relay networks, designing distributed beamforming and relay selection algorithms were extensively studied in [8]–[10]. The approaches were based on e.g. performing the selection by constraining the overall transmit power of the selected relays [8], or by individually constraining their transmit power [9], [10].

After the recent experimental studies that have demonstrated the feasibility of the deployment of FD transceivers [11], [12], more articles have investigated the use of FD transceivers in existing wireless communication applications, where an interesting application of the FD technology was in relaying networks [13]–[19]. A considerable effort has been made to address the fusion of these techniques in which the potential gains and inevitable drawbacks of this fusion were thoroughly investigated. For example, in [13],

an elaborate analysis of various SI cancelation techniques was performed in MIMO-OFDM DF relay networks, where several spatial suppression schemes were presented. In [14], an optimal relay gain that maximizes the end-to-end signal-to-interference-plus-noise ratio (SINR) is derived along with outage probability expressions. Moreover, in [15] and [16], exact outage probability and channel capacity expressions were derived respectively for one-way FD AF relaying network along with optimal single relay selection. Furthermore, in [17], various performance metrics, namely the bit-error rate (BER), outage probability, and the ergodic capacity are derived for two-way FD dual-hop relaying network. Based on these analytical closed-form expressions, single relay selection is performed. Furthermore, the optimal power allocation and the optimal choice of the duplexing scheme (HD or FD mode) were obtained. This hybrid system is also reported in [18] for AF and DF relaying schemes and in [19] for DF relay networks.

Given the available literature, in this article, we study the fusion between FD radio transceivers and AF dual-hop relaying networks. Our contributions are summarized as follows:

- We model the effects of residual SI in a FD AF relay by considering the cumulative SI resulting from the relay operating in a FD mode. Our modeling is based on using the exact varying beamforming coefficient, which is usually modeled as a fixed parameter for the sole purpose of preventing oscillations at the relay [14], [17].
- Assuming the availability of perfect channel-state information (CSI) and second order statics of the residual SI, we design our beamforming coefficient while aiming at minimizing the mean square error (MSE) at the destination, and then utilize sparsity inducing optimization problems to perform relay selection.
- Our proposed beamforming and multiple relay selection technique is shown to be a hybrid FD and alternate relaying system, where we show that the switching rate is mainly dependent on the SI cancelation capability of receivers at the relays.

Paper Organization: The rest of the paper is organized as follows. Section II presents the overall system model. Section III presents a detailed analysis and derivation of the cost function, which will be used in the proposed relay selection and beamfoming techniques. In Section IV, we propose and thoroughly discuss various multiple relay selection and beamforming schemes. In Section V, the numerical results of the proposed techniques are presented, discussed and compared with results from the literature. Finally, the paper is concluded in Section VI.

Notations: The following notations are adopted in the sequel. Unless stated otherwise, upper and lower case bold letters denote matrices and vectors, respectively, $A_{i,j}$ denotes the element in the i^{th} row and j^{th} column of the matrix $\mathbf{A}$, and a_i denotes the i^{th} element of the vector $\mathbf{a}$. The operators $\mathbb{E}\{.\}$, $|.|$ and $(.)^*$ represent the expectation, absolute value and conjugate operators, respectively. For vector and matrices, the operators $(.)^T$, $(.)^H$ and $\odot$ denote the transpose, conjugate-transpose and the element-wise Hadamard product, respectively. For vectors, $||.||_p$, card(.) and $\underset{i\in S}{\overset{K}{\text{argmax}}}(\mathbf{a})$ denote the p^{th}-norm, the cardinality operator, and the arguments of the K largest elements with i being the index of the element for a vector $\mathbf{a}$, respectively.

II. SYSTEM MODEL

The adopted dual-hop wireless network model consists of one source S transmitting data to one destination D with the assistance of N relays, where each relay is denoted by R_i $(i = 1 \dots N)$.

The direct link between the source and the destination is assumed to be unavailable due to severe fading and path-loss. Consequently, the data can be transferred from S to D only through the relays [20]–[23]. To enhance the communication quality between S and D, different techniques are proposed in this paper to select a set of 'best' relays out of the N available relays, based on different selection criteria.

All the relays are assumed to operate in FD mode [17], [15], i.e. each selected relay simultaneously transmits and receives information on the same frequency band, creating SI due to leaking from the previous relay's transmission(s). The channel coefficients for the links $S \rightarrow R_i$ and $R_i \rightarrow D$ are denoted by h_{SR_i} and h_{R_iD}, respectively. The coefficients h_{SR_i} and h_{R_iD} are modeled as complex circularly-symmetric zero-mean Gaussian random variables with variances $\sigma^2_{SR_i}$ and $\sigma^2_{R_iD}$, respectively. Fig. 1 depicts the adopted system model.

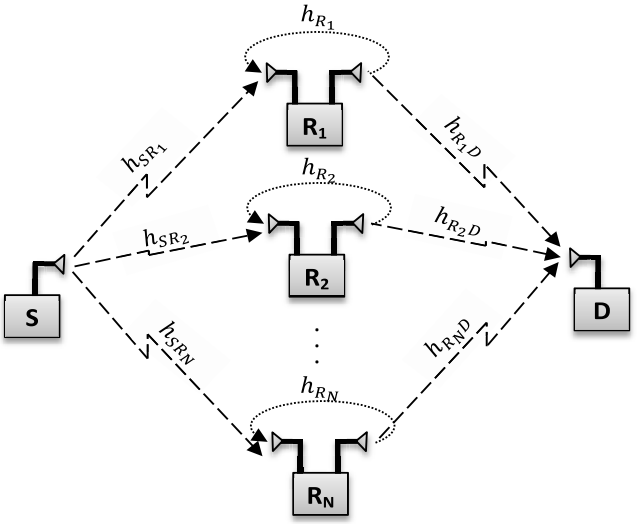

FIGURE 1. System Model.

In the half-duplex case, the selection is dependent on the CSIs between the source and the relay $(S \rightarrow R_i)$ and from the relay to the destination $(R_i \rightarrow D)$ [8], or only their second order statics [9]. However, to guarantee maximum diversity, the selection in FD cooperative networks has to take into consideration the residual SI at each relay, while assuming that each relay is able to cancel some of its SI [15], [17].

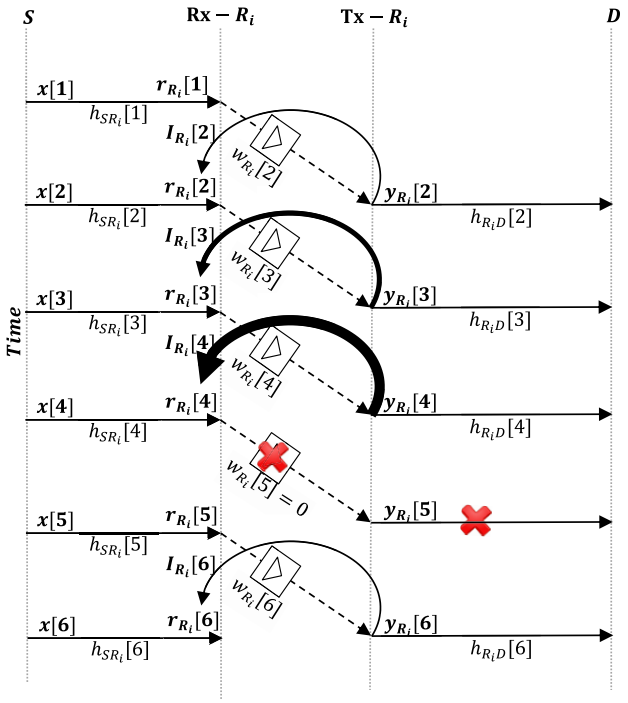

FIGURE 2. Schematic transmission model at the relay R_i.

Fig. 2 represents a detailed schematic drawing of the adopted transmission scheme that a single relay could potentially follow in the network. In particular, during the n^{th} time slot, the source broadcasts the transmitted data $x[n]$ to all the relays. If a relay R_i is selected to forward the data, the received signal $r_{R_i}[n]$ at the i^{th} relay is multiplied by a corresponding beamforming and amplification coefficient $w_{R_i}[n+1]$. The resulting signal $y_{R_i}[n+1]$ is then forwarded in the next time slot to the destination. However, due to the transmission leakage between the Rx and Tx antennas of the relays, SI loops back to the relay's receiver (where the thickness of the SI line represents the severity of the SI). As the SI has a cumulative behavior [14], [17], after some transmission slots (5 transmission slots in Fig. 2), the SI might becomes so high that the diversity brought by that particular relay is low compared to other relays. In this case, it might be better to stop using the relay R_i for at least one time slot to null out the cumulative SI before including it again in the selection set in the next time slot.

In particular, at time slot n, the relay R_i receives the symbol $x[n]$ from the source S, and simultaneously transmits information to the destination D. Therefore, the received signal at the i^{th} relay can be written as

$$r_{R_i}[n] = h_{SR_i}[n]x[n] + v_{R_i}[n] + I_{R_i}[n], \tag{1}$$

where $v_{R_i}[n]$ is an additive-white-Gaussian noise (AWGN) with variance $\sigma^2_{v_{R_i}}$ at the relay R_i in the n^{th} time slot, and $I_{R_i}[n]$ represents the residual SI at the relay R_i in the n^{th} time slot. Furthermore, the residual SI $I_{R_i}[n]$ at time n can be expressed by (See the proof in Appendix A)

$$I_{R_i}[n] = \sum_{m=1}^{n-1}\Big(\prod_{p=n-m+1}^{n}\tilde{h}_{R_i}[p]w_{R_i}[p]\Big) \times\Big(h_{SR_i}[n-m]x[n-m] + v_{R_i}[n-m]\Big), \tag{2}$$

where $\tilde{h}_{R_i}[n]$ represents the residual SI channel [14] modeled as a zero-mean Gaussian random variable with a variance $\sigma^2_{R_i}$ [24]. Note that $\sigma^2_{R_i}$ approaching zero implies that the SI cancelation capability of the relay is high. From (2), we can deduce that the residual SI depends of the SI cancelation capability for each relay and the beamforming coefficients at all the previous time slots. Next, if the relay R_i is selected, a beamforming coefficient $w_{R_i}[n]$ is applied, and the transmitted signal $y_{R_i}[n]$ is then expressed by writing

$$y_{R_i}[n] = w_{R_i}[n]h_{SR_i}[n-1]x[n-1] + w_{R_i}[n]v_{R_i}[n-1] + w_{R_i}[n]I_{R_i}[n-1]. \tag{3}$$

Therefore, the received signal $y_D[n]$ at the destination can be written as

$$y_D[n] = (\mathbf{w}[n])^H\mathbf{a}[n] + v_D[n], \tag{4}$$

where $v_D[n]$ is the AWGN in the n^{th} time slot at the destination with variance $\mathbb{E}\{v_D[n]v^*_D[n]\} = \sigma^2_{v_D}$, and

$$\mathbf{w}[n] \triangleq \Big[w_{R_1}[n], \ldots, w_{R_N}[n]\Big]^H, \tag{5}$$

$$\mathbf{a}[n] \triangleq \Big[a_{R_1}[n], \ldots, a_{R_N}[n]\Big]^H, \tag{6}$$

$$\mathbf{b}[n] \triangleq \Big[b_{R_1}[n], \ldots, b_{R_N}[n]\Big]^H,$$

where $a_{R_i}[n]$ and $b_{R_i}[n]$ are defined by writing

$$\begin{aligned} a_{R_i}[n] &\triangleq h_{R_i,D}[n]h_{S,R_i}[n-1]x[n-1] + h_{R_i,D}[n]v_{R_i}[n-1] \\ &\quad + h_{R_i,D}[n]I_{R_i}[n-1], \\ &= h_{S,R_i,D}[n]x[n-1] + b_{R_i}[n], \end{aligned} \tag{7}$$

and

$$b_{R_i}[n] \triangleq h_{R_iD}[n]v_{R_i}[n-1] + h_{R_iD}[n]I_{R_i}[n-1],$$

where

$$h_{S,R_i,D}[n] \triangleq h_{S,R_i}[n-1] \times h_{R_i,D}[n].$$

From (4), it can be seen that the received signal at the destination depends on the new realizations of $\mathbf{a}$ (h_{SR_i}, h_{R_iD}, $\tilde{h}_{R_i} \mid i = 1..N$) at the current time slot as well as all the previous ones. So, unlike the work in [13] and [17] and to enhance the diversity at the destination, the amplification and beamforming coefficients for each relay should be adapted at each time slot depending on the new realizations.

III. COST FUNCTION ANALYSIS

In this section, we formulate the cost function that will be the performance metric on which our proposed multiple relay selection and beamforming solutions will be based on.

In this work, the cost function is selected to be the MSE as it has been shown for example in [25] and [26] that MSE minimization based selection techniques enhance the BER

performance. Therefore, we next compute the MSE of the received signal $\epsilon[n]$, which can be computed by applying

$$\epsilon[n] \triangleq \mathbb{E}\left\{|x[n-1]-y_D[n]|^2\right\}. \quad (8)$$

Assuming statistical independence between x, v_{R_i} and v_D, we get

$$\begin{aligned}\epsilon[n] &= (\mathbf{w}[n])^H \underbrace{\mathbf{h}_{S,R,D}[n]\mathbf{h}_{S,R,D}^H[n]}_{\triangleq \mathbf{A}[n]}(\mathbf{w}[n])\sigma_x^2 \\ &\quad + (\mathbf{w}[n])^H \underbrace{\mathbb{E}\left\{\mathbf{b}[n](\mathbf{b}[n])^H\right\}}_{\triangleq \mathbf{B}[n]}(\mathbf{w}[n]) + \sigma_D^2 + \sigma_x^2 \\ &\quad - (\mathbf{w}[n])^H \mathbf{h}_{S,R,D}[n]\sigma_x^2 - \mathbf{h}_{S,R,D}^H[n](\mathbf{w}[n])\sigma_x^2. \\ &= (\mathbf{w}[n])^H(\mathbf{A}[n]\sigma_x^2 + \mathbf{B}[n])\mathbf{w}[n] + \sigma_D^2 + \sigma_x^2 \\ &\quad - (\mathbf{w}[n])^H \mathbf{h}_{S,R,D}[n]\sigma_x^2 - \mathbf{h}_{S,R,D}^H[n](\mathbf{w}[n])\sigma_x^2, \quad (9)\end{aligned}$$

where

$$\mathbf{A}[n] \triangleq \mathbf{h}_{S,R,D}[n]\mathbf{h}_{S,R,D}^H[n],$$

and

$$B_{i,j}[n] \triangleq \mathbb{E}\left\{b_{R_i}[n]^* b_{R_j}[n]\right\}, \quad (10)$$

$$= \begin{cases} 0, & \text{if } i \neq j, \\ |h_{R_i,D}[n]|^2\Big(\sigma_v^2 + \sum_{m=1}^{n-2} \\ \times\Big(\prod_{p=n-m}^{n-1}\sigma_{R_i}^2|w_{R_i}[p]|^2\Big) \\ \times\Big(|h_{SR_i}[n-1-m]|^2\sigma_x^2 + \sigma_v^2\Big)\Big), & otherwise. \end{cases}$$

The MSE expression in (9) can be further simplified to

$$\begin{aligned}\epsilon[n] = \mathbf{w}^H[n]\mathbf{R}[n]\,\mathbf{w}[n] - \mathbf{w}^H[n]\mathbf{h}_{S,R,D}[n]\sigma_x^2 \\ -\sigma_x^2\,\mathbf{h}_{S,R,D}^H[n]\mathbf{w}[n] + \sigma_D^2 + \sigma_x^2, \quad (11)\end{aligned}$$

where

$$\mathbf{R}[n] \triangleq \sigma_x^2\mathbf{A}[n] + \mathbf{B}[n]. \quad (12)$$

Using the Cholesky factorization $\mathbf{R}[n] = \mathbf{L}[n]\mathbf{L}^H[n]$, where $\mathbf{L}$ is a lower triangular matrix, we can write

$$\begin{aligned}\epsilon[n] &= \sigma_x^2 + \sigma_D^2 - \mathbf{w}^H[n]\mathbf{L}^{-1}[n]\mathbf{L}[n]\tilde{\mathbf{h}}[n] \\ &\quad - \tilde{\mathbf{h}}^H[n]\mathbf{L}^{-H}[n]\mathbf{L}^H[n]\mathbf{w}[n] \\ &\quad + \mathbf{w}^H[n]\mathbf{L}[n]\mathbf{L}^H[n]\mathbf{w}[n], \quad (13)\end{aligned}$$

where $\tilde{\mathbf{h}}[n] \triangleq \sigma_x^2\mathbf{h}_{S,R,D}[n]$. Consequently, $\epsilon[n]$ can be written in the following form

$$\begin{aligned}\epsilon[n] = \underbrace{\sigma_x^2 - \tilde{\mathbf{h}}^H[n]\mathbf{L}^{-H}[n]\mathbf{L}^{-1}[n]\tilde{\mathbf{h}}[n] + \sigma_D^2}_{\epsilon_{min}[n]} \\ + \underbrace{||\mathbf{L}^H[n]\mathbf{w}[n] - \mathbf{L}^{-1}[n]\tilde{\mathbf{h}}[n]||_2^2}_{\epsilon_{excess}[n]}. \quad (14)\end{aligned}$$

From (14), it can be seen that ϵ_{min} does not depend on $\mathbf{w}[n]$. Consequently, the optimization of $\mathbf{w}[n]$ towards minimizing the MSE at the destination is equivalent to minimizing ϵ_{excess}.

IV. MULTIPLE RELAY SELECTION AND BEAMFORMING SCHEMES

A. PROBLEM FORMULATION

In this work, as we have previously highlighted, we assume that in our system setup, each relay is capable of applying a beamforming coefficient before transmitting to the destination. Further, it has been shown that the problem of selecting k_{max} relays and computing their corresponding beamforming coefficients under total power constraint is expressed by writing

$$\begin{aligned}&\min_{\mathbf{w}} \left(||\mathbf{L}^H[n]\mathbf{w}[n] - \mathbf{L}^{-1}[n]\tilde{\mathbf{h}}[n]||_2^2\right) \\ &\text{s.t. } \text{card}(\mathbf{w}[n]) = k_{max} \\ &\quad \sum_{i=1}^{N} P_{R_i}[n] = \sigma_x^2, \quad (15)\end{aligned}$$

where $k_{max} \in \{1,\ldots,N\}$ represents the number of selected relays, $P_{R_i}[n]$ denotes the transmission power of the relay R_i at the n^{th} time slot and card(.) represents the cardinality function, i.e. the number of non-zero elements in $\mathbf{w}[n]$.

Note that the problem in (15) is an NP-hard problem and requires an exhaustive search over all the possible $\binom{N}{k_{max}}$ combinations, which might be computationally unaffordable [9]. Hence, we next seek to implement computationally affordable algorithms to solve the selection problem.

To simplify the optimization problem in (15), we first focus on selecting the relays and their beamforming coefficients independently from the total transmission power constraint, then -as it will be detailed in Section IV-D- the resulting selection vector is normalized to meet the requirements of the power constraint. Hence, after dropping the power constraint, the selection problem in (15) becomes

$$\begin{aligned}&\min_{\mathbf{w}} \left(||\mathbf{L}^H[n]\mathbf{w}[n] - \mathbf{L}^{-1}[n]\tilde{\mathbf{h}}[n]||_2^2\right) \\ &\text{s.t. } \text{card}(\mathbf{w}[n]) = k_{max}. \quad (16)\end{aligned}$$

B. UNLIMITED NUMBER OF SELECTED RELAYS (UNSR)

In this part, to further reduce the complexity of the problem in (16), the non-convex cardinality constraint is first dropped. In this case, the selection problem can be written as

$$\min_{\mathbf{w}} \left(||\mathbf{L}^H[n]\mathbf{w}[n] - \mathbf{L}^{-1}[n]\tilde{\mathbf{h}}[n]||_2^2\right). \quad (17)$$

1) UNLIMITED NUMBER OF SELECTED RELAYS–ZERO FORCING (UNSR-ZF)

One way to solve the problem (17) is by using the ZF solution given by

$$\mathbf{w}_{ZF}[n] = \mathbf{L}^{-H}[n]\mathbf{L}^{-1}[n]\tilde{\mathbf{h}}[n]. \quad (18)$$

Note that all the elements of the vector $\mathbf{w}_{ZF}[n]$ in (18) are non-zeros which is equivalent to selecting all the relays to forward the data. However, due to the SI cumulative effect,

some relays that suffer from high levels of SI might be requested to transmit with a very small power to null out the cumulative SI before including it again in the selection set in the next time slots, i.e., $\max\left(\mathbf{w}_{ZF}[n]\right) \gg \min\left(\mathbf{w}_{ZF}[n]\right)$. To solve this issue, we propose to exclude the relays that are requested to transmit with a very small power compared to the maximum relay transmission power from the selection set, i.e. $\mathbf{w}_{UNSR-ZF}[n]$ is obtained by nulling the coefficients of $\mathbf{w}_{ZF}[n]$ that satisfy the condition $|\mathbf{w}_{UNSR-ZF}[n]| < \frac{\max(|\mathbf{w}_{UNSR-ZF}[n]|)}{10}$.

2) UNLIMITED NUMBER OF SELECTED RELAYS - ℓ_1-NORM (UNSR-ℓ_1)

Although UNSR-ZF reduces the number of unnecessary relays by excluding the ones that have a very low transmission power, the resulting total number of selected relays might still be more than necessary, i.e. some of the selected relays are using the network resources without providing a significant improvement on the BER performance at the destination. To solve this issue, the ℓ_1-norm sparsifying operator [9] is exploited to force the selection of the least possible number of relays by reformulating the selection to the following optimization problem

$$\begin{aligned} &\min_{\mathbf{w}} \left(||\mathbf{L}^H[n]\mathbf{w}[n] - \mathbf{L}^{-1}[n]\tilde{\mathbf{h}}[n]||_1^2 \right) \\ &\text{s.t. } ||\mathbf{L}^H[n]\mathbf{w}[n] - \mathbf{L}^{-1}[n]\tilde{\mathbf{h}}[n]||_2^2 \leq \delta, \end{aligned} \tag{19}$$

where δ is a threshold predefined by the network administrators corresponding to the minimum acceptable error in ϵ_{excess}. Note that UNSR-ℓ_1 selection technique reduces the number of selected relays compared with UNSR-ZF at the price of higher complexity (optimization problem solving compared to a direct analytical solution). Also, choosing very small values of δ forces the network to use a big number of relays while a bigger δ would require less relays for communications. Consequently, the choice of δ creates a compromise between the MSE performance and the number of selected relays.

C. LIMITED NUMBER OF SELECTED RELAYS (LNSR)

Both UNSR-ZF and UNSR-ℓ_1 techniques aim to minimize the MSE at the destination with a limited number of relays. However, none of them can force the selection of a certain number of active relays in the network which might be impractical in some scenarios. Henceforth, the following presented techniques will guarantee the selection of at most k_{max} relays.

1) LIMITED NUMBER OF SELECTED RELAYS–ZERO FORCING (LNSR-ZF)

We assume in this part that, due to synchronization and implementation challenges, the total number of active relays can not exceed a predefined integer k_{max}, i.e.

$$\begin{aligned} &\min_{\mathbf{w}} \left(||\mathbf{L}^H[n]\mathbf{w}[n] - \mathbf{L}^{-1}[n]\tilde{\mathbf{h}}[n]||_2^2 \right) \\ &\text{s.t. } \text{card}(\mathbf{w}[n]) \leq k_{max}. \end{aligned} \tag{20}$$

To satisfy this condition, the same selection steps of UNSR-ZF are followed. Then, only the k_{max} relays that have the largest $|\mathbf{w}_{LNSR-ZF}[n]|$ are kept active, i.e. the selection set of LNSR-ZF is given by

$$S_{LNSR-ZF} = \underset{i \in 1\ldots N}{\overset{k_{max}}{\text{argmax}}} \left(|\mathbf{w}_{LNSR-ZF}[n]| \right). \tag{21}$$

Then, the same computed beamforming coefficients for UNSR-ZF are kept for LNSR-ZF in the updated selection set, i.e.

$$\mathbf{w}_{LNSR-ZF}[n] = \begin{cases} \mathbf{w}_{UNSR-ZF}[n] & \text{if } i \in S_{LNSR-ZF}[n] \\ 0 & otherwise. \end{cases} \tag{22}$$

2) LIMITED NUMBER OF SELECTED RELAYS - ℓ_1 (LNSR-ℓ_1)

Similar to the UNSR-ℓ_1 technique, the total number of active relays is minimized using ℓ_1-norm squared, then thresholding is performed according to a predefined integer k_{max}, i.e.

$$\begin{aligned} &\min_{\mathbf{w}} \left(||\mathbf{L}^H[n]\mathbf{w}[n] - \mathbf{L}^{-1}[n]\tilde{\mathbf{h}}[n]||_1^2 \right) \\ &\text{s.t. } ||\mathbf{L}^H[n]\mathbf{w}[n] - \mathbf{L}^{-1}[n]\tilde{\mathbf{h}}[n]||_2^2 \leq \delta \\ &\quad \text{card}(\mathbf{w}[n]) \leq k_{max}. \end{aligned} \tag{23}$$

Thus, the only selected relays are the k_{max} relays that have the largest $|\mathbf{w}_{R_i}^{UNSR-\ell_1}[n]|$, i.e.

$$S_{LNSR-\ell_1} = \underset{i \in 1\ldots N}{\overset{k_{max}}{\text{argmax}}} \left(|\mathbf{w}^{UNSR-\ell_1}[n]| \right). \tag{24}$$

The computed beamforming coefficients for UNSR-ℓ_1 are kept for LNSR-ℓ_1 in the updated selection set, i.e.

$$w_{R_i}^{LNSR-\ell_1}[n] = \begin{cases} w_{R_i}^{UNSR-\ell_1}[n] & \text{if } i \in S_{UNSR-\ell_1} \\ 0 & otherwise. \end{cases} \tag{25}$$

D. POWER CONSTRAINT

The power of the signal transmitted from the i^{th} relay $P_{R_{r_i}}$ can be written as

$$\begin{aligned} P_{R_i}[n] &= \mathbb{E}\left\{ |y_{R_i}[n]|^2 \right\} \\ &= |w_{R_i}[n]|^2 \sigma_{S,R}^2 \sigma_x^2 + |w_{R_i}[n]|^2 \sigma_v^2 + |w_{R_i}[n]|^2 \\ &\quad \times \left(\sigma_{S,R}^2 \sigma_x^2 + \sigma_v^2 \right) \sum_{m=1}^{n-1} (\sigma_{R_i}^2)^m \left(\prod_{p=n-m}^{n-1} |w_{R_i}[p]|^2 \right), \end{aligned} \tag{26}$$

where $\sigma_{S,R}^2 = \mathbb{E}\{h_{S,R_i} h_{S,R_i}^*\}$, and $\sigma_R^2 = \mathbb{E}\{h_{R_i} h_{R_i}^*\}$ for $i \in \{1, \ldots, N\}$. Hence, to satisfy the power constraint in (15), the computed beamforming coefficients are multiplied by the following constant

$$\alpha = \frac{\sigma_x^2}{\sum_{i=1}^{N} P_{R_i}[n]}. \tag{27}$$

In this way, the total transmit power from the relays will be equal to σ_x^2.

V. NUMERICAL RESULTS

In this section, the performance of the proposed techniques are simulated and compared with existing techniques in the literature. The performance of these techniques are first evaluated in terms of BER. For better comparison, the average number of selected relays and the relay re-usage percentage are also depicted as metrics to evaluate the performance of the investigated techniques. In particular, the relay re-usage percentage is defined as the average percentage of relays being reused in two consecutive time slots. This metric is used to show how often the network needs to apply switching for the relays that suffer from high residual SI to maintain the desired performance.

TABLE 1. Simulation parameters.

Parameter	Value	Description
N	20	Number of relays.
σ_{SR}^2	0 dB	Variance of $h_{SR_i} \mid i \in \{1, 2, \ldots, N\}$.
σ_{RD}^2	0 dB	Variance of $h_{R_iD} \mid i \in \{1, 2, \ldots, N\}$.
σ_x^2	0 dB	Variance of $x[n] \mid n \in \{1, 2, \ldots, \infty\}$.
n_c	100	Sampled time length at which the CSI is constant.
δ	-15 dB	Minimum acceptable error in ϵ_{excess}.

Table 1 summarizes the adopted simulation configuration parameters, unless stated otherwise in the sequel. In particular, the proposed multiple relay selection techniques are tested for $N = 20$ relays where binary phase-shift keying (BPSK) is used to modulate the data. The BER performance is evaluated for different configurations of the residual SI channel variance ($\sigma_{R_i}^2$), the relay transmit power (σ_x^2) and the maximum number of selected relays (k_{max}). We further assume that the channel coefficients h_{SR_i} and h_{R_iD} $\forall i \in \{1, \ldots, N\}$ are fixed for a certain period of time n_c.[1] Furthermore, we set $\sigma_{SR}^2 = \sigma_{RD}^2 = 0$ dB.

To highlight the gains of our proposed multiple relay selection and beamforming techniques, we compare our approaches with the below existing techniques:

- Optimal Single Relay Selection (OSRS) adopted from [15]: A single relay is selected based on maximizing the SINR at the destination.
- Optimal Single Relay Selection adopted from [15] with beamforming (OSRS-BF): A single relay is selected based on maximizing the SINR at the destination with beamforming applied at the selected relay.

Fig. 3 presents the effect of the residual SI power (by varying $\sigma_{R_i}^2$ $\forall i \in \{1, \ldots, N\}$ from -5 dB to 30 dB) on the performance of the different investigated techniques when the SNR and k_{max} are set to be SNR=3 dB, $k_{max} = 15$.

[1]Note that assuming that the channel coefficients are varying at each time slot and that their realizations are perfectly known by the source might not be practical in some networks. That's why the channel coefficients h_{SR_i} and h_{R_iD} are assumed to be slowly varying and change after n_c time slots.

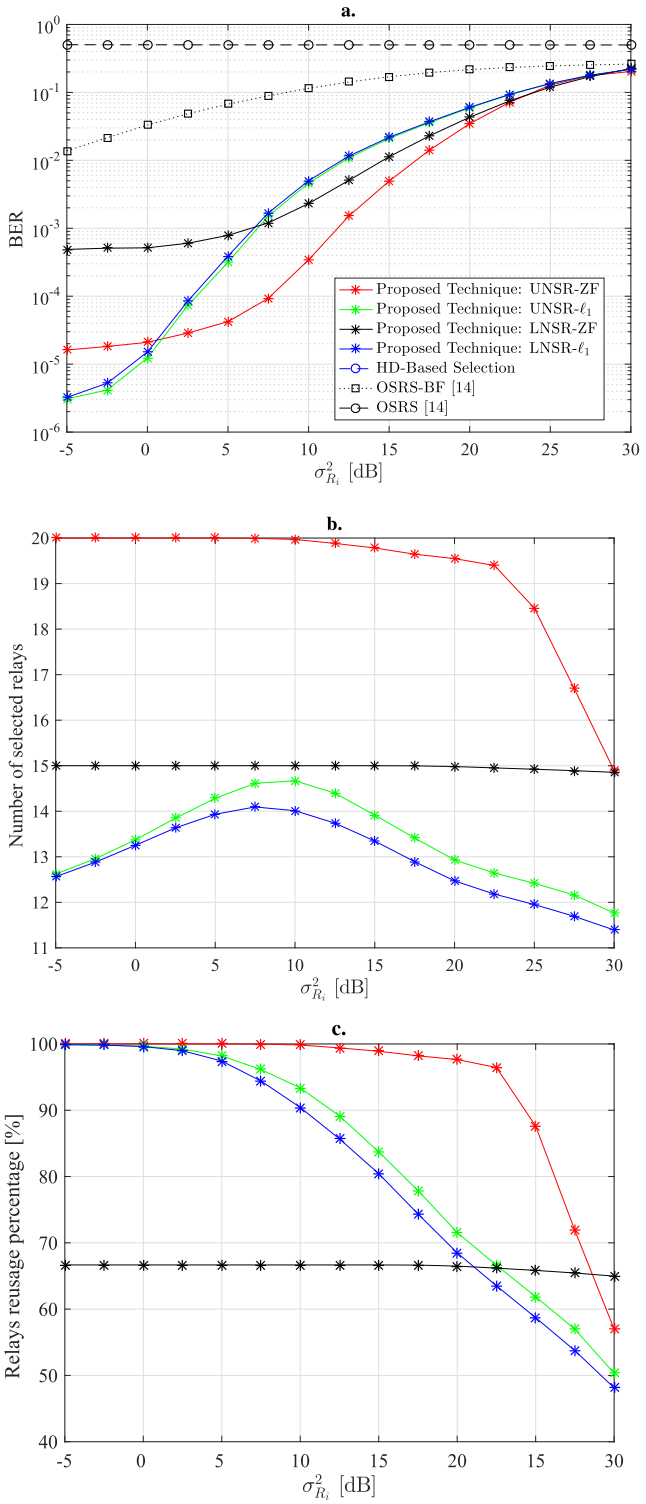

FIGURE 3. The behavior of different relaying strategies as a function of $\sigma_{R_i}^2$: a. Average BER vs. $\sigma_{R_i}^2$. b. Average number of selected relays relays vs. $\sigma_{R_i}^2$. c. Average relay re-usage percentage vs. $\sigma_{R_i}^2$.

First, it can be seen that the proposed techniques LNSR-ZF, UNSR-ZF, LNSR-ℓ_1 and UNSR-ℓ_1 outperform the OSRS technique presented in [15] even when beamforming is applied to it (OSRS-BF). This is, in part, due to the fact

that the method in [15] selects only a single relay and that the proposed techniques in this paper allow the network to switch between relays at each time slot, if necessary.

Note also that OSRS selection technique provides a high BER at these ranges of parameters compared to the remaining techniques because, in addition to selecting only a single relay, no beamforming is applied.

For low $\sigma_{R_i}^2$, the LNSR-ℓ_1 and UNSR-ℓ_1 perform the best with the lowest number of relays, especially for low values of δ, at the price of an increased complexity (optimizaion problem solving instead of direct ZF solution) compared to ZF techniques. However, the UNSR-ZF technique starts performing better than all other techniques as $\sigma_{R_i}^2$ increases. This is explained by looking at Fig. 3-b where the depicted results show the average number of selected relays as a function of $\sigma_{R_i}^2$. The results reveal that the UNSR-ZF method uses a larger number of selected relays as it focuses on minimizing the MSE more than reducing the number of selected relays. Note that, although up to 20 relays can be used by UNSR-ZF and UNSR-ℓ_1, and up to 15 relays can be used by LNSR-ZF and LNSR-ℓ_1, the average number of selected relays is much less than those used for very high values of SI. In particular, for high values of SI, no big difference can be seen between the BER of the different techniques (see Fig. 3-a) as the system performance is almost saturated. Hence, the proposed techniques automatically decide that using more relays will not be of great benefit to the MSE performance and therefore a smaller number of relays is used. On the other hand, the optimization in UNSR-ℓ_1 and LNSR-ℓ_1 have a target MSE to reach with the minimum possible number of relays. Hence, obviously, increasing the SI level will require from the system to use more relays to reach this target until a value of SI (around 10 dB) where the target MSE is no longer reached anyway. At this point, the number of used relays by UNSR-ℓ_1 and LNSR-ℓ_1 techniques start to decrease by the effect of ℓ_1-norm minimization.

Furthermore, the relay re-usage percentage is depicted in Fig. 3-c as a function of $\sigma_{R_i}^2$. The LNSR-ZF technique has almost a fixed relay re-usage rate of about 67%. However, our other proposed UNSR-ZF and UNSR-ℓ_1 based methods are shown to be very responsive to $\sigma_{R_i}^2$. Note that the re-usage rate is fixed at 100% when $\sigma_{R_i}^2$ is low and could reach about 48% when $\sigma_{R_i}^2$ is high, i.e. when there is a very limited level of interference, there is no need to switch between the relays. Hence, we can understand that when the level of SI is very high, reusing the same relays becomes more difficult because of the cumulative effect of the SI. Therefore, depending on the SI level, the proposed techniques dynamically decide whether there is a benefit or not from switching the transmission between the relays and how often this should be done given that switching might create few implementation and synchronization challenges and therefore should be avoided when not beneficial.

In Fig. 4-a, the BER performance is plotted against the source and the relay's transmit power ($P = \sigma_x^2 = P_{R_i}[n]$), while the SNR is set to be 10 dB and $\sigma_{R_i}^2 = 15$ dB.

Note that the UNSR-ZF technique shows the best BER performance compared to other techniques but while using the biggest number of selected relays as depicted in Fig. 4-b (20 relays are used and then the number drops after $P = 22$ dBm). Note that all the investigated techniques suffer from an error floor starting from some specific value of transmit power. In particular, increasing the transmit power enhances the SNR level but also increases the SI at the relays and deteriorates the performance. Hence, starting from 25 dBm, increasing the transmit power -almost- does not affect the BER performance.

We observe that for the UNSR-ℓ_1 and LNSR-ℓ_1 techniques, the number of selected relays starts increasing as P increases, and then revert to decreasing when $P > 20$ dBm for the UNSR-ℓ_1 method and when $P > 24$ dBm for the LNSR-ℓ_1 method. This is due to the fact that increasing the transmit power at the relays increases the SI, and the system decides to use less relays to mitigate the SI's detrimental effect on the overall BER performance. Moreover, we note that the LNSR-ℓ_1 technique has the lowest number of selected relays as shown in Fig. 4-b. The OSRS method has a very high BER since BF is not applied, while the OSRS-BF performs better than the OSRS method, although it performs worse than the other proposed techniques due to only selecting one relay.

Fig. 4-c shows the re-usage percentage of the selected relays, and shows that the UNSR-ℓ_1 method is the most responsive to the variation of P, decreasing at a very fast rate when $P > 20$ dBm. The LNSR-ZF method has a re-usage percentage which is fixed at around 67%, and then starts decreasing when $P > 26$ dBm. Both the UNSR-ℓ_1 and the UNSR-ZF have higher re-usage percentages, while the UNSR-ℓ_1 technique starts becoming very responsive when $P > 20$ dBm after being constant at 100 % re-usage percentage. In particular, Fig. 4-c confirms that the proposed techniques and especially UNSR-ℓ_1 and LNSR-ℓ_1 can dynamically maximize the percentage of re-usage depending on the transmit power to keep the required performance whenever possible.

In Fig. 5-a, the BER performance is depicted against k_{max} for SNR=10 dB and $\sigma_{R_i}^2 = 15$ dB. Without beamforming, the OSRS technique has high BER while with beamforming, the BER performance is enhanced and performs considerably better, although the rest of the proposed techniques outperform it as k_{max} increases. It can be seen also that increasing the maximum number of selected relays k_{max} increases the diversity level and reduces the BER of the limited number of selected relays techniques (LNSR-ZF and LNSR-ℓ_1). Further, both the LNSR-ℓ_1 and UNSR-ℓ_1 techniques reach a saturation level after around 13 relays are selected as increasing the number of relays would not enhance the performance. In particular, such kind of saturation is often seen in relay selection schemes as in e.g. [9]. Normally, by allowing UNSR-ℓ_1 to use up to 20 relays compared to LNSR-ℓ_1 which is allowed to use up to k_{max} relays with the same beamforming coefficients, UNSR-ℓ_1 should always perform better than LNSR-ℓ_1. However, it can be seen that LNSR-ℓ_1

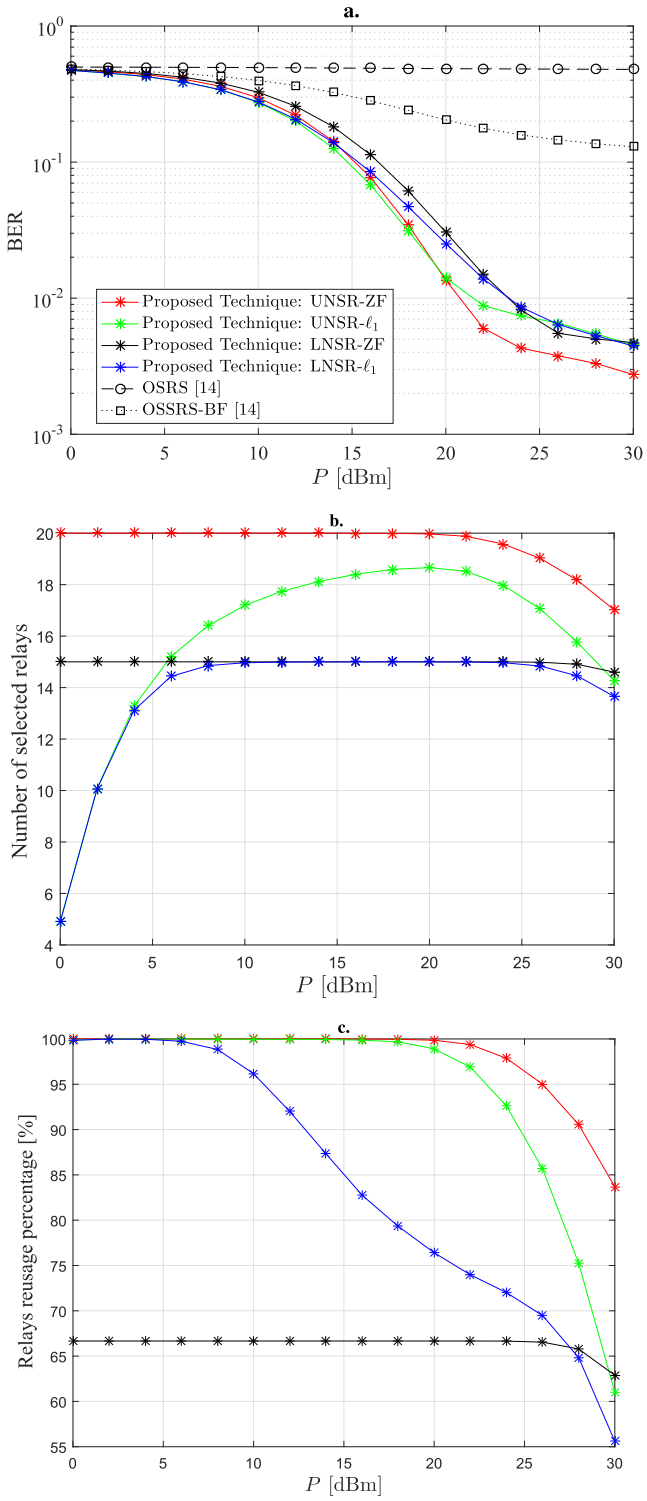

FIGURE 4. The behavior of different relaying strategies as a function of P: a. Average BER vs. P. b. Average number of selected relays relays vs. P. c. Average relay re-usage percentage vs. P.

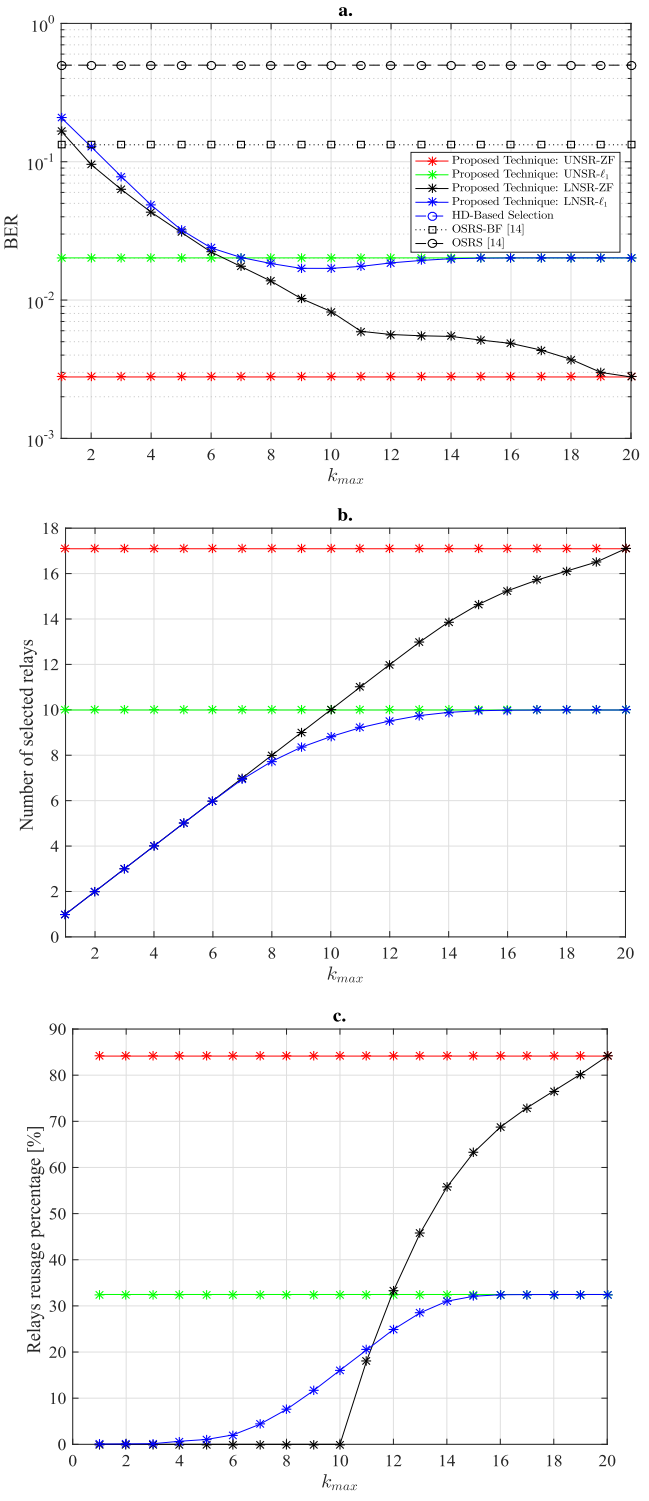

FIGURE 5. The behavior of different relaying strategies as a function of k_{max}: a. Average BER vs. k_{max}. b. Average number of selected relays relays vs. k_{max}. c. Average relay re-usage percentage vs. k_{max}.

has slightly higher BER performance compared to UNSR-ℓ_1 technique from around $k_{max} = 8$ to $k_{max} = 12$ relays. This is due to the thresholding step at the end of UNSR-ℓ_1 and LNSR-ℓ_1 techniques intended to reduce the number of used relays which is indeed a low complexity but not optimal solution. From Fig. 5-b, both UNSR-ℓ_1 and LNSR-ℓ_1 use almost the same number of selected relays when k_{max} is around 13.

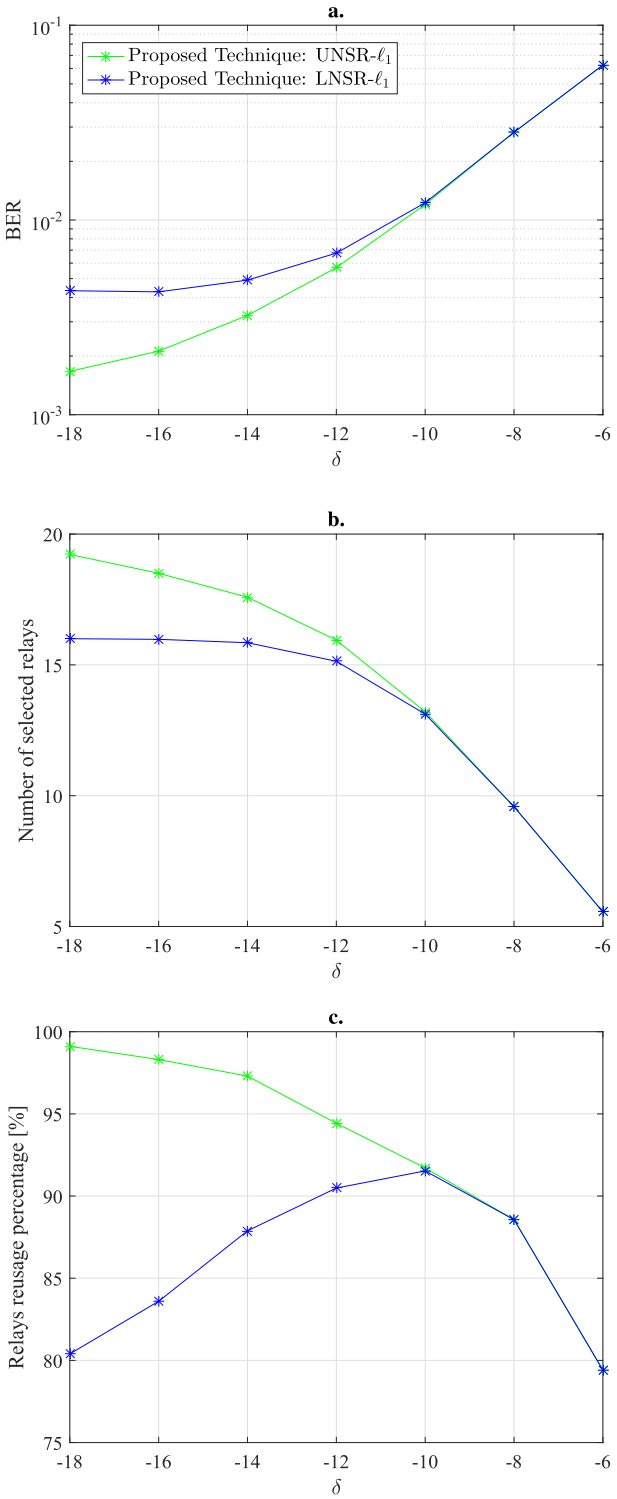

FIGURE 6. The behavior of the proposed UNSR-ℓ_1 and LNSR-ℓ_1 relay selection techniques as a function of δ: **a.** Average BER vs. δ. **b.** Average number of selected relays relays vs. δ. **c.** Average relay re-usage percentage vs. δ.

For the cases of the UNSR-ZF and LSNR-ZF, UNSR-ZF is always performing much better than its LNSR-ZF counterpart at the expense of always using more relays.

In Fig. 5-c, the re-usage percentage is plotted as a function of k_{max} for all the proposed techniques. It can be noticed that all the techniques that are designed to be a function of k_{max} are very responsive to the relay re-usage percentage and adaptively decide on how often the relays should switch based on the maximum allowed number of relays.

Lastly, concerning the effect of the constant δ that bounds the inequalities for the constraints in (19) and (23), the BER, the average number of selected relays and the average relay re-usage percentage are all plotted against δ in Fig. 6-a, Fig. 6-b and Fig. 6-c, respectively. The simulations were performed for an SNR of 2 dB, $\sigma_{R_i}^2 = 12$ dB and for $k_{max} = 16$. The proposed selection techniques that are used to generate the results are UNSR-ℓ_1 and LNSR-ℓ_1, since both of the selection problems depend on the constant δ, which was varied between -18 dB and -4 dB. These results are provided to highlight the effect of δ besides the fact that it has an effect on the complexity of the proposed selection techniques. The results show that in general, the BER performances of both the UNSR-ℓ_1 and LNSR-ℓ_1 selection techniques depend on δ since both techniques show better performances when δ is small and the performance deteriorates as the value of δ increases. This behavior can be explained by the fact that tightening the bound in the constraints in (19) and (23) results in a better BER performance. Furthermore, the UNSR-ℓ_1 technique outperforms the performance of its LNSR-ℓ_1 counterpart in the interval that is around -18 dB $< \delta < -10$ dB since as depicted in Fig. 6-b, the average number of selected relays for the LNSR-ℓ_1 technique saturates at $k_{max} = 16$, while the average number of selected relays for the UNSR-ℓ_1 selection technique keeps increasing, hence providing a better BER performance. In Fig. 6-c, the average relay re-usage percentage increases as δ gets smaller for the UNSR-ℓ_1 technique since the average number of selected relays is also increased, making the usage of the same relay inevitable. However, for the LNSR-ℓ_1 selection technique, the average relay re-usage percentage increases from 80% to around 93% when δ goes from -18 dB until -10 dB and then drops again to around 78% when δ reaches -6 dB. When δ is relatively high, the number of selected relays for both the UNSR-ℓ_1 LNSR-ℓ_1 techniques is low (as only a limited number of relays can satisfy the constraint in (19) and (23)). Hence, the UNSR-ℓ_1 and LNSR-ℓ_1 techniques provide almost the same solution and therefore the same number of relays and relay re-usage percentage. Note that the relay re-usage percentage decreases when δ goes from -10 dB until -6 dB as the number of selected relays for the UNSR-ℓ_1 and LNSR-ℓ_1 techniques also decreases. However, for small values of δ (form around -18 dB to -14 dB), the average number of selected relays for the LNSR-ℓ_1 technique saturates at $k_{max} = 16$, forcing the LNSR-ℓ_1 technique to drop the relay re-usage percentage to avoid the SI and maintain an acceptable BER performance.

VI. CONCLUSION

Novel multiple relay selection schemes for AF FD dual-hop relay networks that utilizes sparsity inducing optimization problems towards minimizing the MSE level were presented.

Based on the accurate modeling of the cumulative SI at each relaying node, our algorithms adopt a hybrid strategy involving FD and switching approaches to avoid the high SI interference at each relay node, and hereby improve the overall system performance in terms of BER. A compromise between BER performance, number of used relays and selection complexity is created between the different proposed techniques. We have also captured the level of hybridity of our proposed algorithm by simulating the relay re-usage rate as a function of an the SI level, transmit power and number of relays. The proposed techniques showed their high efficiency and demonstrated that they can dynamically decide when and how often the transmission should be switched from one relay to another to keep the desired performance.

.

APPENDIX A
PROOF OF (2) BY RECURSION

We now proceed to prove the correctness of (2) by using a recursion approach. Recalling that the received signal $r_{R_i}[n]$ at the relay R_i is written as

$$r_{R_i}[n] = h_{SR_i}[n]x[n] + v_{R_i}[n] + I_{R_i}[n]. \quad \text{(A.28)}$$

The residual SI $I_{R_i}[n+1]$ at time instant $n+1$ can be written as

$$\begin{aligned} I_{R_i}[n+1] &= \tilde{h}_{R_i}[n+1]w_{R_i}[n+1]r_{R_i}[n], \\ &= \tilde{h}_{R_i}[n+1]w_{R_i}[n+1] \\ &\quad \times \Big(h_{SR_i}[n]x[n] + v_{R_i}[n] + I_{R_i}[n]\Big), \\ &= \alpha[n+1]\Big(\beta[n] + I_{R_i}[n]\Big). \end{aligned} \quad \text{(A.29)}$$

where $\alpha[n] = \tilde{h}_{R_i}[n]w_{R_i}[n]$ and $\beta[n] = h_{SR_i}[n]x[n] + v_{R_i}[n]$. Note that when $n = 1$, the relay does not suffer from SI, i.e. $I_{R_i}[1] = 0$. This is true since the relay starts transmitting at time slot 1.

Next, we prove by recurrence that (2) is correct $\forall n$. When using the notation in (A.29), $I_{R_i}[n]$ is written as

$$I_{R_i}[n] = \sum_{m=1}^{n-1}\Big(\prod_{p=n-m+1}^{n}\alpha[p]\Big)\beta[n-m]. \quad \text{(A.30)}$$

When $n = 2$, (A.30) is expanded by writing

$$\begin{aligned} I_{R_i}[2] &= \sum_{m=1}^{2-1}\Big(\prod_{p=2-m+1}^{2}\alpha[p]\Big)\beta[n-m] \\ &= \alpha[2]\beta[1]. \end{aligned} \quad \text{(A.31)}$$

Since $I_{R_i}[1] = 0$, we deduce from (A.31) and (A.29) that (A.30) is verified when $n = 2$. Next, assuming (A.30) is correct for n, (A.30) needs to be verified also for $n+1$. In particular, we deduce from (A.29) that

$$\begin{aligned} &I_{R_i}[n+1] \\ &= \alpha[n+1]\Big(\beta[n] + I_{R_i}[n]\Big), \end{aligned} \quad \text{(A.32)}$$

$$= \alpha[n+1]\Big(\beta[n] + \sum_{m=1}^{n-1}\Big(\prod_{p=n-m+1}^{n}\alpha[p]\Big)\beta[n-m]\Big), \quad \text{(A.33)}$$

$$= \alpha[n+1]\beta[n] + \sum_{m=1}^{n-1}\Big(\prod_{p=n-m+1}^{n+1}\alpha[p]\Big)\beta[n-m]. \quad \text{(A.34)}$$

Applying the change of variables $q = m+1$, we proceed to write

$$\begin{aligned} I_{R_i}[n+1] &= \alpha[n+1]\beta[n] \\ &\quad + \sum_{q=2}^{n}\Big(\prod_{p=n-q+2}^{n+1}\alpha[p]\Big)\beta[n-q+1], \\ &= \sum_{q=1}^{n}\Big(\prod_{p=n-q+2}^{n+1}\alpha[p]\Big)\beta[n-q+1], \end{aligned} \quad \text{(A.35)}$$

which is equal to (A.30) for the $n+1$'s time slot. This concludes our proof.

REFERENCES

[1] A. Sabharwal, P. Schniter, D. Guo, D. W. Bliss, S. Rangarajan, and R. Wichman, "In-band full-duplex wireless: Challenges and opportunities," *IEEE J. Sel. Areas Commun.*, vol. 32, no. 9, pp. 1637–1652, Sep. 2014.

[2] V. Syrjala, M. Valkama, L. Anttila, T. Riihonen, and D. Korpi, "Analysis of oscillator phase-noise effects on self-interference cancellation in full-duplex OFDM radio transceivers," *IEEE Trans. Wireless Commun.*, vol. 13, no. 6, pp. 2977–2990, Jun. 2014.

[3] L. Samara, M. Mokhtar, Ö. Özdemir, R. Hamila, and T. Khattab, "Residual self-interference analysis for full-duplex OFDM transceivers under phase noise and I/Q imbalance," *IEEE Commun. Lett.*, vol. 21, no. 2, pp. 314–317, Feb. 2017.

[4] D. Korpi, L. I. Anttila, and V. Syrjälä, and M. Valkama, "Widely linear digital self-interference cancellation in direct-conversion full-duplex transceiver," *IEEE J. Sel. Areas Commun.*, vol. 32, no. 9, pp. 1674–1687, Sep. 2014.

[5] J. I. Choi, M. Jain, K. Srinivasan, P. Levis, and S. Katti, "Achieving single channel, full duplex wireless communication," in *Proc. 16th Annu. Int. Conf. Mob. Comput. Netw.*, 2010, pp. 1–12.

[6] A. Sendonaris, E. Erkip, and B. Aazhang, "User cooperation diversity. Part I. System description," *IEEE Trans. Commun.*, vol. 51, no. 11, pp. 1927–1938, Nov. 2003.

[7] A. Sendonaris, E. Erkip, and B. Aazhang, "User cooperation diversity. Part II. Implementation aspects and performance analysis," *IEEE Trans. Commun.*, vol. 51, no. 11, pp. 1939–1948, Nov. 2003.

[8] V. Havary-Nassab, S. Shahbazpanahi, A. Grami, and Z.-Q. Luo, "Distributed beamforming for relay networks based on second-order statistics of the channel state information," *IEEE Trans. Signal Process.*, vol. 56, no. 9, pp. 4306–4316, Sep. 2008.

[9] L. Blanco and M. Nájar, "Sparse multiple relay selection for network beamforming with individual power constraints using semidefinite relaxation," *IEEE Trans. Wireless Commun.*, vol. 15, no. 2, pp. 1206–1217, Feb. 2016.

[10] A. Gouissem, L. Samara, R. Hamila, N. Al-Dhahir, and S. Foufou, "Relay selection in FDD amplify-and-forward cooperative networks," in *Proc. IEEE 28th Annu. Int. Symp. Pers., Indoor, Mobile Radio Commun. (PIMRC)*, Oct. 2017, pp. 1–7.

[11] D. Bharadia, E. McMilin, and S. Katti, "Full duplex radios," *ACM SIGCOMM Comput. Commun. Rev.*, vol. 43, no. 4, pp. 375–386, Sep. 2013.

[12] M. Duarte *et al.*, "Design and characterization of a full-duplex multiantenna system for WiFi networks," *IEEE Trans. Veh. Technol.*, vol. 63, no. 3, pp. 1160–1177, Mar. 2014.

[13] T. Riihonen, S. Werner, and R. Wichman, "Mitigation of loopback self-interference in full-duplex MIMO relays," *IEEE Trans. Signal Process.*, vol. 59, no. 12, pp. 5983–5993, Dec. 2011.

[14] T. Riihonen, S. Werner, and R. Wichman, "Optimized gain control for single-frequency relaying with loop interference," *IEEE Trans. Wireless Commun.*, vol. 8, no. 6, pp. 2801–2806, Jun. 2009.

[15] I. Krikidis, H. A. Suraweera, P. J. Smith, and C. Yuen, "Full-duplex relay selection for amplify-and-forward cooperative networks," *IEEE Trans. Wireless Commun.*, vol. 11, no. 12, pp. 4381–4393, Dec. 2012.

[16] P. C. Sofotasios, M. K. Fikadu, S. Muhaidat, S. Freear, G. K. Karagiannidis, and M. Valkama, "Relay selection based full-duplex cooperative systems under adaptive transmission," *IEEE Wireless Commun. Lett.*, vol. 6, no. 5, pp. 602–605, Oct. 2017.

[17] H. Cui, M. Ma, L. Song, and B. Jiao, "Relay selection for two-way full duplex relay networks with amplify-and-forward protocol," *IEEE Trans. Wireless Commun.*, vol. 13, no. 7, pp. 3768–3777, Jul. 2014.

[18] T. Riihonen, S. Werner, and R. Wichman, "Hybrid full-duplex/half-duplex relaying with transmit power adaptation," *IEEE Trans. Wireless Commun.*, vol. 10, no. 9, pp. 3074–3085, Sep. 2011.

[19] T. Kwon, S. Lim, S. Choi, and D. Hong, "Optimal duplex mode for DF relay in terms of the outage probability," *IEEE Trans. Veh. Technol.*, vol. 59, no. 7, pp. 3628–3634, Sep. 2010.

[20] Z. Chen, L. X. Cai, Y. Cheng, and H. Shan, "Sustainable cooperative communication in wireless powered networks with energy harvesting relay," *IEEE Trans. Wireless Commun.*, vol. 16, no. 12, pp. 8175–8189, Dec. 2017.

[21] Z. Yi and I.-M. Kim, "Optimum beamforming in the broadcasting phase of bidirectional cooperative communication with multiple decode-and-forward relays," *IEEE Trans. Wireless Commun.*, vol. 8, no. 12, pp. 5806–5812, Dec. 2009.

[22] A. Alsharoa, H. Ghazzai, A. E. Kamal, and A. Kadri, "Optimization of a power splitting protocol for two-way multiple energy harvesting relay system," *IEEE Trans. Green Commun. Netw.*, vol. 1, no. 4, pp. 444–457, Dec. 2017.

[23] B. V. Nguyen and K. Kim, "Single relay selection for secure communication in a cooperative system with multiple full-duplex decode-and-forward relays," in *Proc. IEEE Int. Workshop Inf. Forensics Secur. (WIFS)*, Nov. 2015, pp. 1–6.

[24] W. Cheng, X. Zhang, and H. Zhang, "Optimal dynamic power control for full-duplex bidirectional-channel based wireless networks," in *Proc. IEEE INFOCOM*, Apr. 2013, pp. 3120–3128.

[25] J. Lee and N. Al-Dhahir, "Exploiting sparsity for multiple relay selection with relay gain control in large AF relay networks," *IEEE Wireless Commun. Lett.*, vol. 2, no. 3, pp. 347–350, Jun. 2013.

[26] A. Gouissem, R. Hamila, N. Al-Dhahir, and S. Foufou, "A sparsity-aware approach for NBI estimation and mitigation in large cognitive radio networks," in *Proc. IEEE 84th Veh. Technol. Conf. (VTC-Fall)*, Sep. 2016, pp. 1–7.

LUTFI SAMARA received the B.Sc. degree in electrical engineering from Qatar University, Doha, Qatar, in 2011, and the M.Sc. degree in information technology from the Tampere University of Technology, Tampere, Finland, in 2013. He is currently pursuing the Ph.D. degree in electrical engineering with the Department of Electrical Engineering, Qatar University. His current research interests include modeling and compensation of radio frequency impairments in radio transceivers and cooperative communications.

ALA GOUISSEM received the bachelor's and master's degrees in telecommunications from the Higher School of Communications of Tunisia (Sup'Com) in 2011 and 2013, respectively, and the Ph.D. degree in computer science from the University of Burgundy, Dijon, France, in 2017. He is currently a Researcher with the Department of Electrical Engineering, Qatar University, Doha, Qatar. His current research interests are in the general areas of signal processing, wireless communications, energy saving and especially the statistical approaches of cooperative communication, OFDM transmissions, compressive sensing, and data center architectures.

RIDHA HAMILA received the M.Sc. degree, the Lic. Tech. degree (Hons.), and the Dr. Tech. degree from the Tampere University of Technology (TUT), Tampere, Finland, in 1996, 1999, and 2002, respectively. From 1994 to 2002, he held various research and teaching positions with the Department of Information Technology, TUT. From 2002 to 2003, he was a System Specialist with the Nokia Research Center, Helsinki, and also with Nokia Networks, Helsinki. From 2004 to 2009, he was with Emirates Telecommunications Corporation, UAE. From 2004 to 2013, he was an Adjunct Professor with the Department of Communications Engineering, TUT. He is currently a Full Professor with the Department of Electrical Engineering, Qatar University, Doha, Qatar. His current research interests include mobile and broadband wireless communication systems, PHY security, and machine learning.